AMSE JOURNALS-AMSE IIETA publication-2017-Series: Advances C; Vol. 72; N°1; pp 48-66
Submitted Jan. 2017; Revised March 15, 2017, Accepted April 15, 2017
https://doi.org/10.18280/ama_c.720104

Singular Value Decomposition aided Robust Cubature Quadrature Kalman Filter in GPS/INS Integrated Navigation System

Wei Zhao, Huiguang Li, Liying Zou

School of Electrical Engineering, Yanshan University, Qinhuangdao 066004, China

(zhwei19800@163.com, ysulihuiguang@163.com, zouliying2007@126.com)

Abstract

The paper presents a singular value decomposition aided H-∞ Cubature Quadrature Kalman filter (SVD-HCQKF) in GPS/INS integrated navigation system to satisfy the high requirements of the precision and robustness of aircraft integrated navigation system. The Cubature Quadrature Kalman filter (CQKF) uses the hyper-sphere cubature rule and two-order Gauss-Laguerre quadrature rule to generate Cubature Quadrature points to calculate multiple moment integral that is different from the Cubature Kalman filter (CKF) using cubature points. The robustness of the system is also guaranteed by the addition of the H-∞ algorithm. In numerical simulation, it is verified that the accuracy and robustness of the proposed algorithm and SVD aided CQKF are better than those under CKF frame. Finally, the proposed algorithm is applied in GPS/INS integrated navigation system, and the simulation results show it can greatly improve the accuracy and robustness of the system.

Keywords

Integrated navigation system, Robust filter, Cubature Quadrature Kalman filter, Singular value decomposition

1. Introduction

For aircraft navigation system, there are a variety of options, such as the global positioning system (GPS), BeiDou navigation satellite system (BDS), inertial navigation system (INS), Doppler navigation system (DNP), etc.. Among these systems, GPS and INS are the most common. The GPS calculates the position and the speed of the aircraft according to the received navigation satellite signals, and has good positioning accuracy, but its anti-disturbance ability is poor. The INS relies entirely on its own sensors to get the position and speed information with strong anti-interference ability, but the navigation error will accumulate over time [1]. So the main idea of GPS/INS integral navigation system is to combine the two systems to make best use of their advantages and bypass their disadvantages, which will improve the overall performance of the navigation system. Now GPS/INS integral navigation system is the world's recognized best solution [2].

The integrated navigation system using Kalman filter is termed optimal integrated navigation system [3]. As an important part of the integrated navigation system, Kalman fiter uses probability statistics to estimate the error of the navigation system in the optimal angle to correct the system. For decades, the optimal integrated navigation system has been developed greatly, and a lot of filtering algorithms under the Kalman filter framework arise for improving the positioning accuracy. The most simple and common used algorithm is the extended Kalman filter (EKF) in integral navigation system [4]. Due to the EKF using the first-order Taylor expansion, it is obviously insufficient for the high performance of precision navigation. Then the people put forward unscented Kalman filter (UKF)[5], Cubature Kalman filter (CKF)[6], particle filter (PF)[7] algorithm to improve the performance of the integrated navigation system. In [8], a UKF-based integrated navigation for GPS/INS provides precise position and orientation to the photogrammetric adjustment. In turn, the photogrammetric adjustment provides position updates to the UKF. The CKF filtering principle is applied as the INS/GPS integrated filter in [9] to simulate nonlinear model based on the platform misalignment angle and the observation model described by the velocity error and position error. The literature [10] presents a new particle filter algorithm and this new filter uses the difference filter and the latest observed measurements to generate the importance-density in the importance sampling.

In [11], Sahoo and Dash give the Cubature Quadrature Kalman filter (CQKF) algorithm, which is the more generalized form of CKF. The difference of CQKF compared to CKF is mainly reflected in a more accurate calculation method for the numerical integration. In CQKF, the multiple moment integration is divided into two parts, the surface integral over an *n*-dimensional hyper-sphere which could be calculated using spherical cubature rule and the line integral which could be evaluated using the *n*'-order Gauss-Laguerre quadrature rule of integration. When *n*'=1, the accuracy of CQKF generally coincides with the CKF. The accuracy of the filter depends on the order of Gauss-Laguerre quadrature rule. The higher the order, the more accurate the estimator would be. In addition, the CQKF with 2*nn*' sampling points has better computational efficiency than the PF with 2*n*^*n* sampling points, and slightly higher than the UKF with 2*n*+1 points and CKF with 2*n* points [12].

In order to deal with indeterminacy data involving uncertainty and randomness, robust algorithm is investigated by many scholars [13]. H-∞ filter introduces the H_2 norm into the filtering problem, and build a filter to minimize the H_2 norm from the input of disturbance to the output of filter error, so that minimize estimation error under the worst case of interference. In recent years, in order to overcome the uncertainty of the system or gross errors, many scholars combines H-∞ with these nonlinear filtering algorithms, such as EKF [14], UKF [15] and CKF [16], in integrated navigation system.

While using the Cholesky decomposition during the process of filtering using CKF or CQKF, the covariance matrix P may lose positive definite affected by the abnormal situation. The use of alternative corresponding matrix through singular value decomposition to replace covariance matrix of cubature points as characteristics covariance matrix can improve the stability of numerical calculation.

In this paper we design a singular value decomposition aided H-∞ Cubature Quadrature Kalman Filter (SVD-HCQKF) in GPS/INS integrated navigation system where the two-order Gauss-Laguerre quadrature rules is applied to improve the filtering accuracy compared to the SVDCKF. At the same time, the H-∞ filtering algorithm can also enhance the robustness of the system.

The organization of the remaining part is as follows: Section2 introduces the principle of

GPS/INS integrated navigation system and establishes its discrete mathematics model by the analysis of the error models of the system; In dection3, after introducing the basic principle of H-∞ and calculation method for cubature quadrature points (CQ points), the SVD-HCQKF algorithm is given. The numerical simulation and GPS/ins navigation system simulation with analysis are shown in section4; Conclusions are made in section 5.

2. The principle and mathematical model of GPS/INS integrated navigation system

2.1 The principle of GPS/INS integrated navigation system

According to the different requirements of the application level, there are two categories of GPS/INS integrated navigation system, the tight coupling and the loose coupling system.. The tight coupling system is characterized by design of two systems (GPS and INS) together as one. However, the two systems work independently in the loose coupling system, which makes the structure simple and easy to achieve, and GPS in here only plays the role of auxiliary to INS. In this paper, the loose coupling GPS/INS integrated navigation system is used.

In the loose coupling system, the difference of position and velocity information between the outputs of GPS and INS is used as the output of the Kalman filter. Then the filter can estimate the error of inertial navigation system, and realize the correction of the INS. The principle diagram of the loose coupling system is as shown in Fig. 1.

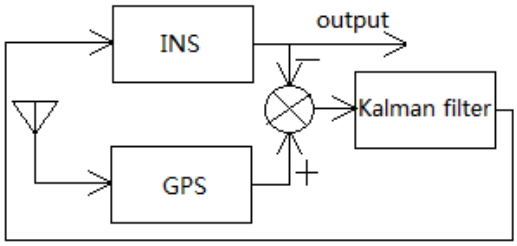

Fig.1 The principle diagram of the loose coupling GPS/INS integrated navigation system

2.2 Mathematical model of GPS/INS integrated navigation system

As mentioned before, the GPS/INS integrated navigation system uses the system error

between GPS and INS as the state. In this paper, we select the 18 errors as the filter state, which consists of the following four parts.

1. The platform error angles: the pitch angle Φ_E, the roll angle Φ_N and the heading angle Φ_U

When the flying height of the aircraft is h and the earth is a rotating ellipsoid, we have

$$\Phi_E = -\frac{\delta V_N}{R_M + h} + (w_{ie}\sin L + \frac{V_E}{R_N + h}tgL)\Phi_N - (w_{ie}\cos L + \frac{V_E}{R_N + h})\Phi_U + \varepsilon_U \tag{1}$$

$$\Phi_N = \frac{\delta V_E}{R_N + h} - w_{ie}\delta L\sin L - (w_{ie}\sin L + \frac{V_E}{R_N + h}tgL)\Phi_E - \frac{V_E}{R_M + h}\Phi_U + \varepsilon_N \tag{2}$$

$$\Phi_N = \frac{\delta V_E}{R_N + h}tgL + (w_{ie}\cos L + \frac{V_E}{R_N + h}\sec^2 L)\delta L + (w_{ie}\cos L + \frac{V_E}{R_N + h})\Phi_E + \frac{V_N}{R_M + h}\Phi_U + \varepsilon_U \tag{3}$$

where $R_M = R_e(1-2f+3f\sin^2 L)$ is the curvature radius of each points at the principal vertical circle of the reference ellipsoid. $R_N = R_e(1+f\sin^2 L)$ is the curvature radius of each points at the prime vertical circle of the reference ellipsoid of the earth. R_e, w_{ie} and f are the long radius, the angular velocity and the oblateness of the earth, respectively.

2. The velocity errors: the error of east velocity δV_E, the error of north velocity δV_N, the error of up velocity δV_U

$$\begin{aligned}\delta V_E = {} & f_N\Phi_U - f_U\Phi_N + (\frac{V_N}{R_M + h}tgL - \frac{V_U}{R_M + h})\delta V_E + (2w_{ie}\sin L + \frac{V_E}{R_N + h}tgL)\delta V_N \\ & + (2w_{ie}V_N\cos L + \frac{V_E V_N}{R_N + h}\sec^2 L + 2w_{ie}V_U\sin L)\delta L - (2w_{ie}V_N\cos L + \frac{V_E}{R_N + h})\delta V_U + \nabla_E\end{aligned} \tag{4}$$

$$\begin{aligned}\delta V_N = {} & f_U\Phi_E - f_E\Phi_U + (2w_{ie}\sin L + \frac{V_N}{R_N + h}tgL)\delta V_E - \frac{V_U}{R_M + h}\delta V_N \\ & - \frac{V_N}{R_M + h}\delta V_U - (2w_{ie}\cos L + \frac{V_E}{R_N + h}\sec^2 L)V_E\delta L + \nabla_N\end{aligned} \tag{5}$$

$$\begin{aligned}\delta V_U = {} & f_E\Phi_N - f_N\Phi_E + (2w_{ie}\cos L + \frac{V_E}{R_N + h})\delta V_E + 2\frac{V_N}{R_M + h}\delta V_N \\ & - 2w_{ie}V_E\delta L\sin L + \nabla_U\end{aligned} \tag{6}$$

3. The position errors: the latitude error δL, the longitude error $\delta\lambda$ and the height error δh

$$\dot{\delta L} = \frac{\delta V_N}{R_M + h} \tag{7}$$

$$\dot{\delta \lambda} = \frac{\delta V_E}{R_N + h} \sec L + \frac{\delta V_E}{R_N + h} \delta L \sec L tgL \tag{8}$$

$$\dot{\delta h} = \delta V_U \tag{9}$$

4. The gyro drift errors: the gyro drifts of three axial, ε_{bx}, ε_{by} and ε_{bz}, and the first-order Markov process drift of three axial, ε_{rx}, ε_{ry} and ε_{rz}

The gyro drift is usually taken as

$$\varepsilon = \varepsilon_b + \varepsilon_r + w_g \tag{10}$$

where w_g is the white noise.

Assuming the gyro drift error models of three axial are the same, they can be obtained as follow

$$\dot{\varepsilon}_b = 0 \tag{11}$$

$$\dot{\varepsilon}_r = -\frac{1}{T_g} \varepsilon_r + w_r \tag{12}$$

where T_g is the relevant time, and w_r is the white noise.

5. The accelerometer errors: the accelerometer errors of three axial, ∇_x, ∇_y and ∇_z

Assuming that the accelerometer error models of three axial are the same. Taking ∇_x for example, it can be expressed as

$$\dot{\nabla}_x = -\frac{1}{T_g} \nabla_x + w_x \tag{13}$$

where T_g is the relevant time, and w_x is the white noise.

As a result, the state of the GPS/INS integrated navigation system can be set as

$$\begin{aligned} x = [&\Phi_E \quad \Phi_N \quad \Phi_U \quad \delta V_E \quad \delta V_N \quad \delta V_U \quad \delta L \quad \delta \lambda \quad \delta h \\ &\varepsilon_{bx} \quad \varepsilon_{by} \quad \varepsilon_{bz} \quad \varepsilon_{rx} \quad \varepsilon_{ry} \quad \varepsilon_{rz} \quad \nabla_x \quad \nabla_y \quad \nabla_z]^T \end{aligned} \tag{14}$$

According to Eqs. (1) - (14), the state equation of GPS/INS integrated navigation system can

be obtained. The general time-continuous form of the system can be expressed as

$$x(t) = F(t)x(t) + G(t)\omega(t) \tag{15}$$

where $F(t)$, $G(t)$ and $\omega(t)$ are the state equation, measurement equation, and process noise, respectively.

The observation object are the east, north and up position errors and velocity errors of in the integral navigation system, and the corresponding measurement equation can be obtained in Eq.(16).

$$y(t) = H(t)x(t) + v(t) \tag{16}$$

where $H(t)$ is the measurement matrix, and $v(t)$ is the measurement noise.

The corresponding discrete model is obtained by discretization of the time-continuous model of Eq.(15) and Eq.(16).

$$x_{k+1} = A_k x_k + B_k \omega_k \tag{17}$$

$$y_{k+1} = C_k x_{k+1} + v_k \tag{18}$$

where $\omega_k \sim N(0, Q_k)$ is the process noise, and $v_k \sim N(0, R_k)$ is the measurement noise.

The above two equations Eq.(17) and Eq.(18) are the discrete model of GPS/INS integrated navigation system used in this paper.

3 The SVD aided robust CQKF

3.1 The principle of H-∞ filtering algorithm

Taking into account the above discrete system, assume that the vector to be estimated is

$$z_{k+1} = L_{k+1} x_{k+1} \tag{19}$$

where L_{k+1} is known.

Define the cost function as follow

$$J = \frac{\sum_{k=0}^{n} \left\| z_{k+1} - \hat{z}_{k+1} \right\|^2}{(x_0 - \hat{x}_0) P_0^{-1} (x_0 - \hat{x}_0)^T + (\sum_{k=0}^{n} \omega_k^T Q_k^{-1} \omega_k + v_k^T R_k^{-1} v_k)} \tag{20}$$

where $\wedge$ denotes the estimated value of the corresponding matrix.

H-∞ filtering for z_{k+1} can be converted to calculate $\hat{z}_{k+1}$ that satisfies the inequality.

$$\sup J \le \gamma^2 \tag{21}$$

where γ is the specified boundary constraint level.

Alternatively, γ should meet the Raccati inequality.

$$P_{k+1}^{-1} + C_k^T C_k - \gamma^2 L_{k+1}^T L_{k+1} > 0 \tag{22}$$

where P_{k+1} is the covariance matrix of state x_{k+1}.

The value of γ affects the accuracy and robustness of the H-∞ filter. If γ approaches infinity, H-∞ filter will be simplified to Kalman filter. The smaller γ, the better the robustness would be. If γ is too small, however, sometimes the Raccati inequality is no longer valid, resulting in that the H-∞ filter does not exist. Generally we will give a determinate constraint level, which leads to the H-∞ filter may not reach the optimal and in fact become a suboptimal filter. So in the actual use of H-∞ control, we can continue to reduce the value of γ to make the suboptimal filter approach to the solution of the optimal H-∞ filter.

3.2 Cubature quadrature points and their corresponding weights

The CQKF algorithm uses hyper-sphere cubature rule and multiple orders Gauss-Laguerre quadrature rule to generate cubature quadrature points (CQ points) to calculate the moment integral. More precisely, the supported CQ points and the corresponding weights approximate the integrals by weighted sum of the functions evaluated at those points. It is obtained by the product of CQ points and their corresponding weights to approximate the product of multiple moments. The multiple moment integration is divided into two parts, the surface integral and the line integral. The first integral is over an n-dimensional hyper-sphere which could be calculated using spherical cubature rule, while the other could be evaluated using the *n*'-order Gauss-Laguerre quadrature rule of integration.

The step for calculating cubature quadrature points and their corresponding weights is as follow

1) According to the dimension of state, give the cubature points $[1]_i$, $i = 1,2,...2n$.

where $[1]_i$ is the *i*-th column of the points set $[1]$.

2) Solve the *n*'-order Chebyshev-Laguerre polynomial in Eq.(23) to obtain the quadrature points λ_j, $j = 1,2,...n'$.

$$L_{n'}^{\alpha}(\lambda) = \lambda^{n'} - \frac{n'}{1!}(n'+\alpha)\lambda^{n'-1} + \frac{n'(n'-1)}{2!}(n'+\alpha)(n'+\alpha-1)\lambda^{n'-2} - ... = 0 \tag{23}$$

3) Obtain the CQ points and calculate their corresponding weights w_k, $k = 1,2,...,2nn'$.

$$\zeta_k = \sqrt{2\lambda_j}[1]_i \tag{24}$$

$$w_k = \frac{1}{2n\Gamma(n/2)} \frac{n'!\Gamma(\alpha+n'+1)}{\lambda_j \left[\dot{L}_{n'}^{\alpha}(\lambda_j) \right]^2} \tag{25}$$

where $\alpha = n/2 - 1$.

When *n* and *n*' are determined, the CQ points and their corresponding weights are determined too. Taking the numerical simulation to be carried out for the 4-dimension system for example, when the two-order Gauss-Laguerre quadrature rule is adopted, the results of 16 CQ points and their corresponding weights are calculated in Eq.(26) and Eq.(27), respectively.

$$\begin{bmatrix} 3.0764 * I_4 & -3.0764 * I_4 & 1.5929 * I_4 & -1.5929 * I_4 \end{bmatrix} \tag{26}$$

$$[0.0265 * ones(1,8) \quad 0.0986 * ones(1,8)] \tag{27}$$

3.3 The SVD-HCQKF algorithm

In the CQKF or CKF algorithms, the covariance matrix *P* may lose positive definite when using the Cholesky decomposition. So the use of alternative corresponding matrix through singular value decomposition can improve the stability of numerical calculation. These algorithms here are called SVD aided CQKF (SVD-CQKF) and SVD aided CKF (SVD-CKF), respectively. Through the analysis in 3.1 and 3.2, the SVD aided H-∞ CQKF algorithm, referred to as SVD-HCQKF, is given below.

A. initialization

1) Initialize with $\hat{x}_0 = E(x_0)$ and $\hat{P}_{x,0} = E((x_0 - \hat{x}_0)(x_0 - \hat{x}_0)^T)$

2) Obtain the CQ points and calculate their corresponding weights by Eqs.(23)-(25)

2. Time update

1) Obtain the new CQ points by singular value decomposition for $\hat{P}_{x,k}$.

$$\hat{P}_{x,k} = U_k \begin{bmatrix} S_k^* & 0 \\ 0 & 0 \end{bmatrix} V_k^T \tag{28}$$

$$\hat{X}_{i,k} = U_k \sqrt{S_k^*}\xi_i + \hat{x}_k \qquad i = 1,2.....2nn' \tag{29}$$

2) These CQ points are propagated through the state equation shown in Eq.(30).

$$\hat{X}_{i,k+1/k} = A_k \hat{X}_{i,k} \tag{30}$$

3) Calculate the value of state prediction $\hat{x}_{k+1/k}$, and covariance matrix $\hat{P}_{x,k+1/k}$.

$$\hat{x}_{k+1/k} = \sum_{i=1}^{2nn'} w_i \hat{X}_{i,k+1/k} \tag{31}$$

$$\hat{P}_{x,k+1/k} = \sum_{i=1}^{2nn'} w_i (\hat{X}_{i,k+1/k} - \hat{x}_{k+1/k})(\hat{X}_{i,k+1/k} - \hat{x}_{k+1/k}) + B_k * Q_k * B_k^T \tag{32}$$

3. Measurement update

1) Obtain the new CQ points by singular value decomposition for $\hat{P}_{x,k+1/k}$.

$$\hat{P}_{x,k+1/k} = U_k \begin{bmatrix} S_k^* & 0 \\ 0 & 0 \end{bmatrix} V_k^T \tag{33}$$

$$\hat{X}^*_{i,k+1/k} = U_k \sqrt{S_k^*}\xi_i + \hat{x}_{k+1/k} \qquad i = 1,2.....2nn' \tag{34}$$

2) These CQ points are propagated through the measurement equation.

$$\hat{Y}_{i,k+1/k} = C_{k+1} \hat{X}^*_{i,k+1/k} \tag{35}$$

3) Calculate the measurement estimation.

$$\hat{y}_{k+1/k} = \sum_{i=1}^{2nn'} w_i \hat{Y}_{i,k+1/k} \tag{36}$$

4) Calculate the measurement prediction $\hat{P}_{y,k+1/k}$ and cross-covariance matrix $\hat{P}_{xy,k+1/k}$.

$$\hat{P}_{y,k+1/k} = \sum_{i=1}^{2nn'} w_j (\hat{Y}_{i,k+1/k} - \hat{y}_{k+1/k})(\hat{Y}_{i,k+1/k} - \hat{y}_{k+1/k})^T + R_k \tag{37}$$

$$\hat{P}_{xy,k+1/k} = \sum_{i=1}^{2nn'} w_j (\hat{X}^{*}_{i,k+1/k} - \hat{x}_{k+1/k})(\hat{Y}_{i,k+1/k} - \hat{y}_{k+1/k})^T \tag{38}$$

4. State update

1) The observer gain K_{k+1} can be obtained as

$$K_{K+1} = \hat{P}_{xy,k+1/k}\, \hat{P}_{yy,k+1/k} \tag{39}$$

2) Calculate the state estimation.

$$\hat{x}_{k+1} = \hat{x}_{k+1/k} + K_{k+1}(y_{k+1} - \hat{y}_{k+1/k}) \tag{40}$$

3) Calculate covariance matrix for H-∞ filtering.

$$\hat{P}_{x,k+1} = \hat{P}_{x,k+1/k} - \begin{bmatrix} \hat{P}_{xy,k+1/k} & \hat{P}_{x,k+1/k} \end{bmatrix} \begin{bmatrix} \hat{P}_{y,k+1/k} - R_k + I & \hat{P}^{T}_{xy,k+1/k} \\ \hat{P}_{xy,k+1/k} & \hat{P}_{x,k+1/k} - \gamma^2 I \end{bmatrix}^{-1} \begin{bmatrix} \hat{P}^{T}_{xy,k+1/k} \\ \hat{P}^{T}_{x,k+1/k} \end{bmatrix} \tag{41}$$

4. Simulation and analysis

4.1Numerical simulation and analysis

In this section, we use a high non-linear model to simulate and verify the effectiveness of the proposed algorithm. The system is described as follows.

$$\begin{cases} X_1(k+1) = 0.001(d(k)z(k) - e(k)b(k))/c(k) + X_1(k) + \omega_1(k) \\ X_2(k+1) = 0.001(-e(k)z(k) - a_3 b(k))/c(k) + X_2(k) + \omega_2(k) \\ X_3(k+1) = 0.001 X_1(k) + X_3(k) + \omega_3(k) \\ X_4(k+1) = 0.001 X_2(k) + X_4(k) + \omega_4(k) \end{cases} \tag{42}$$

where

$z(k) = 2.12\sin(X_4(k))(X_1(k)X_2(k) + 0.5X_2^2(k)) - 81.82\cos(X_3(k)) - 24.6\cos(X_3(k) + X_4(k)) + u_1(k)$,

$b(k) = -1.06\sin(X_4(k)) - 24.6\cos(X_3(k) + X_4(k)) + u_2(k)$, $c(k) = 0.71d(k) - e^2(k)$, $d(k) = 3.82 + 2.12\cos(X_4(k))$,

$e(k) = 0.71 + 1.06\cos(X_4(k)), u_1(k) = 120 + 5\exp(-0.2k))$, $u_2(k) = 115 + 10\exp(-0.2k))$,

The process noise $\omega(k) \sim N(0, Q)$ with zero-mean and the covariance Q.

$$Q = diag([0.1, 0.1, 0.1, 0.1]) \tag{43}$$

The measurement equation is shown in Eq.(44).

$$\begin{cases} y_1(k+1) = X_1(k+1)X_3(k+1) + \upsilon_1(k+1) \\ y_2(k+1) = X_2(k+1) + \upsilon_2(k+1) \\ y_3(k+1) = X_3(k+1) + 0.5X_4(k+1) + \upsilon_3(k+1) \end{cases} \tag{44}$$

where the measurement noise $v(k) \sim N(0, R)$ with zero-mean and the covariance R.

$$R = \text{diag}([0.01, 0.01, 0.01]) \tag{45}$$

Before filtering, the true values of $X(0)$ is $[-0.2, 0.1, 0.1, 0.1]^{\mathrm{T}}$, the initial estimated values of $\hat{X}^{+}(0)$ is $[0, 0, 0., 0]^{\mathrm{T}}$, the initial associated covariance $P(0) = \text{diag}([1,1,1,1])$.

While to estimate the state of X_2, the four algorithms, SVD-CKF, SVD-CQKF, SVD-HCKF and SVD-HCQK, are used in two scenes. These two kinds of scenes are that the system has the uncertainty or not.

Scene1: System with no uncertainty

The estimations of X_2 by the four algorithms are shown in Fig. 2. The constraint level γ of SVD-HCKF and SVD-HCQKF is equal to 2. As can be seen in Fig.2, each of the four algorithms can be a good estimation of X_2. The root mean square error (RMSE) of estimated X_2 can be seen in Table 1. The RMSE using SVD-CQKF with two-order Gauss-Laguerre quadrature rule is slightly smaller than that of the SED-CKF. Due to the introduction of γ, the RMSE is much higher in SVD-HCKF and SVD-HCQKF algorithm for the system without uncertainty. We can also see that the SVD-HCQKF has a higher accuracy relative to SVD-CKF.

Table 1. RMSE of X_2 in numerical simulation

Algorithm	RMSE of X_2	
	Scene1	Scene2
SVD-CKF	0.1719	3.9144
SVD-CQKF	0.1708	3.4660
SVD-HCKF(γ=2)	0.2204	1.569
SVD-HCQKF(γ=2)	0.2185	1.219

In order to analyze the accuracy for these four algorithms, the RMSE of estimated X_2 with different γ in scene 1 is as shown in Table2. We can adjust γ to reduce the RMSE, and get the

same conclusion in Table 1.

Table 2. RMSEs of X_2 with different γ

Algorithm	RMSE of X_2								
	γ=0.1	γ=0.13	γ=0.25	γ=0.5	γ=1	γ=2	γ=5	γ=50	γ=100
SVD-HCKF in Scene1	0.1836	0.1751	0.2118	0.2812	0.3015	0.2204	0.2134	0.2032	0.2032
SVD-HCQKF in Scene1	0.1813	0.1742	0.2114	0.2805	0.2972	0.2185	0.2057	0.2032	0.2032
SVD-HCKF in Scene2	4.1530	3.3545	1.8177	0.5374	0.4407	1.569	2.1767	1.6345	1.6358
SVD-HCQKF in Scene2	3.7788	3.2008	1.3514	0.5026	0.3982	1.219	1.5403	1.6161	1.6174

Scene2: System with uncertainty that X_2 increased by 50 during instant 50-150

Fig. 3 shows the estimation of X_2 by the four algorithms when the uncertainty happens in the system. It is not difficult to see that the robust algorithms (SVD-HCKF and SVD-HCQKF) have better robustness compared to the other two algorithms in scene2. The RMSE of estimated X_2 with different γ in scene 2 is also shown in Table2 in which the RMSEs of two kinds of robust algorithms are much smaller, and especially SVD-HCQKF shows the best accuracy in four methods.

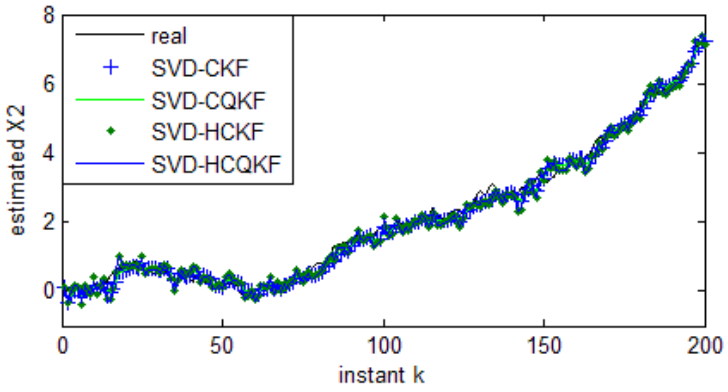

Fig.2 The estimated X_2 in scene1 (γ=2)

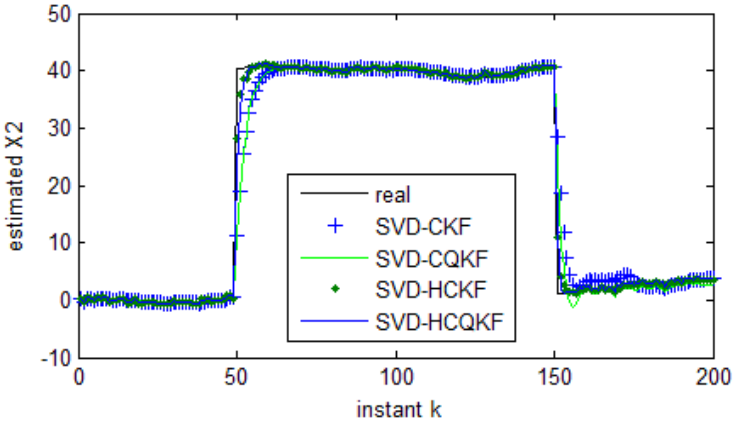

Fig.3 The estimated X_2 in scene2(γ=2)

4.2 Simulation and analysis in GPS/INS integrated navigation system

Assume that the initial position of an aircraft is at 5000 meters altitude with latitude 30° and longitude 110°. The initial pitch angle, roll angle and heading angle are 5°, 50°and 0°, respectively. The gyro constant drift is 0.01°/h, the constant zero offset of accelerometer is 10^{-4}g, and the random zero offset is 10^{-3}g. The aircraft flies 500 seconds from the initial position with 10m/s. The trajectory parameter table with the changed parameters in the motion process is shown in Table 3, and the other parameters that do not arise in the table are unchanged. The Actual flight path is shown in Fig. 4.

Figs.5-10 draw out the curves of the east, north and up position error and velocity error using SVD-CKF and SVD-HCQKF (γ=1.5) in GPS/INS integral navigation system. It can be seen that the accuracy of estimated errors by SVD-CQKF is better than SVD-CKF. In addition, the Table 4 gives RMSE of the errors, and also shows that the filtering effect of SVD-HCQKF for the integrated navigation system is very good where the RMSE of the east, north and up velocities are reduced by 5.4%, 10.1% and 8.6% compared to SVD-CKF, respectively.

Table 3. The trajectory parameter table at time t

t(s)	pitch(º)	head(º)	roll(º)
0-100	5	50	0
101-110	5+(t-100)	50+(t-100)	0
111-210	15	60	0

211-220	15-0.5*(t-211)	15+0.5*(t-211)	0
221-500	5	55	0

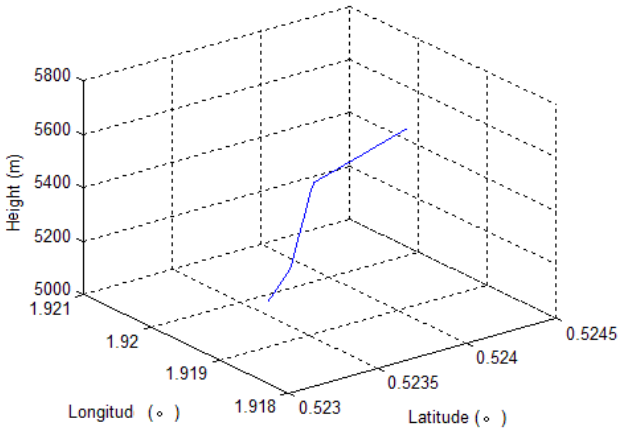

Fig.4 The actual flight path

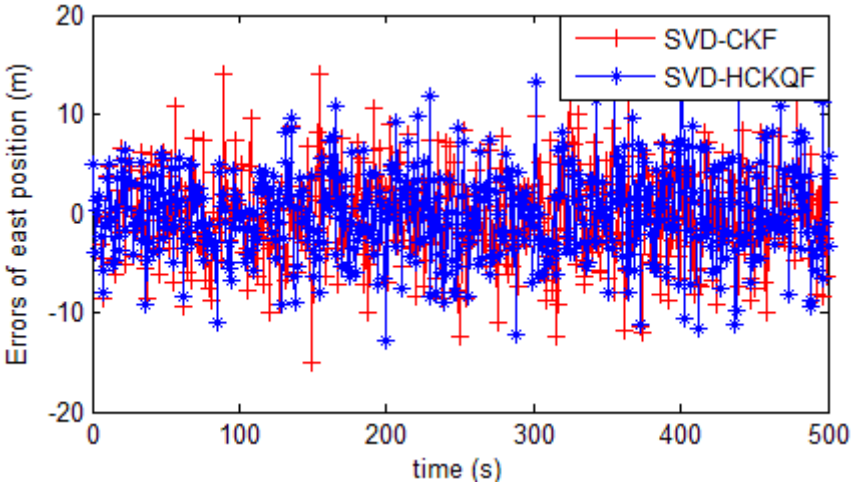

Fig.5 Error of east position

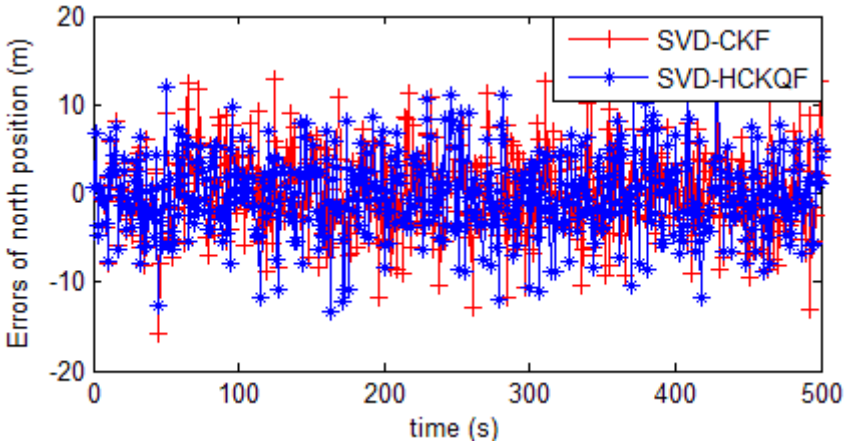

Fig.6 Error of north position

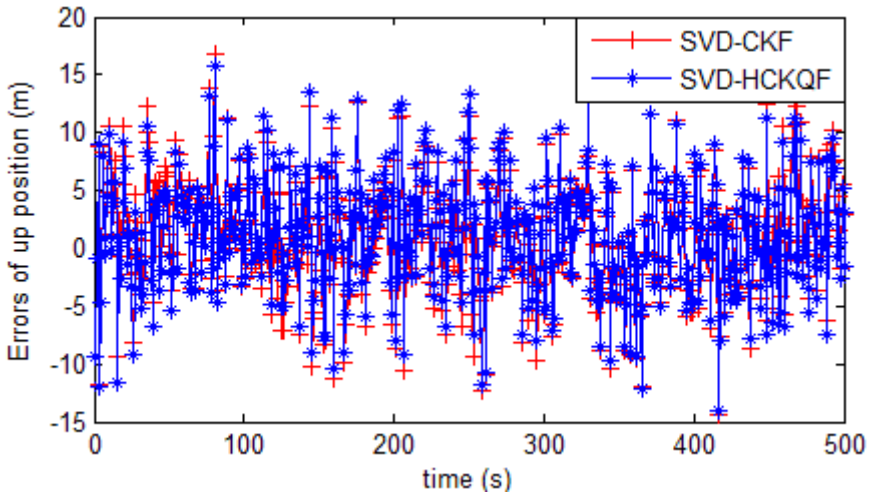

Fig.7 Error of up position

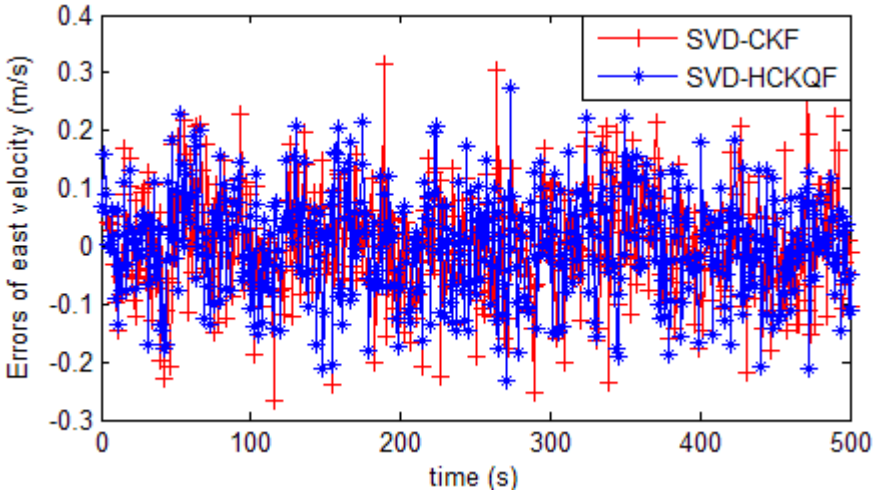

Fig.8 Error of east velocity

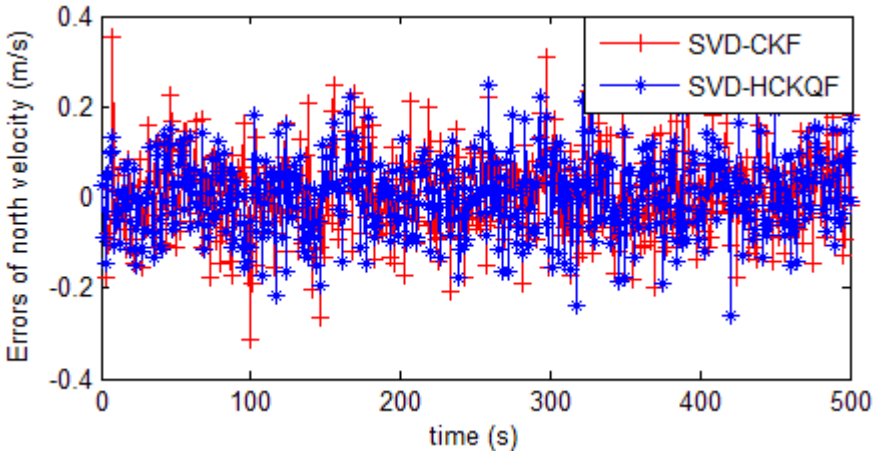

Fig.9 Error of north velocity

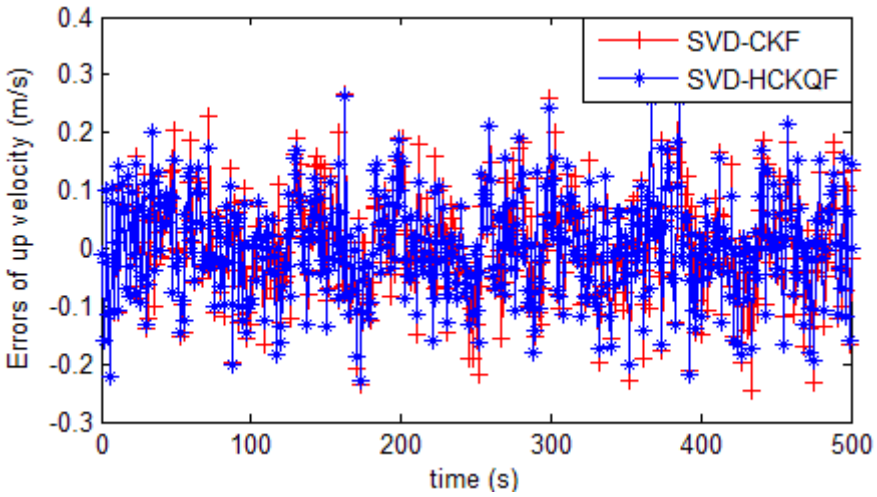

Fig.10 Error of up velocity

Table 4. RMSEs of positions and velocities in GPS/INS simulation

State	RMSE	
	SVD-CKF	SVD-HCQKF (γ=1.5)
Error of east position (m)	4.8009	4.601
Error of north position (m)	4.8616	4.6296
Error of up position (m)	5.2759	5.2357
Error of east velocity(m/s)	0.0967	0.0915
Error of north velocity (m/s)	0.0949	0.0853
Error of up velocity (m/s)	0.0962	0.0879

5. Conclusion

In this paper a robust filtering algorithm, SVD-HCQKF, is designed for the GPS/INS integrated navigation. The proposed algorithm uses hyper-sphere cubature rule and two-order Gauss-Laguerre quadrature rule to generate CQ points to calculate the moment integral, which can improve the accuracy of the filter. At the same time, the application of H-∞ algorithm enhances the robustness of the proposed algorithm. Simulation results show that the SVD-HCQKF has a good robustness to the system uncertainties, and the filtering accuracy is

significantly improved compared with the SVD-CKF, SVD-HCKF and other algorithms. Due to the influence of γ on the robust algorithm, how to choose the optimal constraint level γ is the work that needs further research.

Reference

1. M. Malleswaran, V. Vaidehi, N. Sivasankari. A novel approach to the integration of GPS and optimization INS using recurrent neural networks with evolutionary techniques, 2014, Aerospace Science & Technology, vol. 32, no. 1, pp.169-179.
2. K.T. Leung, J.F. Whidborne, D. Purdy, P. Barber, Road vehicle state estimation using low-cost GPS/INS, 2011, Mechanical Systems & Signal Processing, vol. 25, no. 6, pp.1988-2004.
3. A. Farrell, M. Barth, The global positioning system and inertial navigation, 1999, New York: McGraw-Hill, pp.102-129.
4. P. Ye, X.Q. Zhan, Y.H. Zhang, Mended EKF-Based GPS/INS Tight Coupling Simulator, 2011, Advanced Materials Research, no. 271-273, pp.609-615.
5. M. Gupta, L. Behera, V.K. Subramanian, M.M. Jamshidi, A Robust Visual Human Detection Approach With UKF-Based Motion Tracking for a Mobile Robot, 2014, IEEE Systems Journal, no.4, pp.1-13.
6. W. Zhao, H.G. Li, L.Y. Zou, and R.H. Yuan, Aaptive and robust single value decomposition aided cubature kalman filter with chi-square test, 2016, Control and Intelligent Systems, vol. 44, no. 1, pp.36-43.
7. T. Yang, R.S. Laugesen, P.G. Mehta, S.P. Meyn, Multivariable feedback particle filter, 2016, Automatica, vol.71, no.1, pp.10-23.
8. X. Zhai, F. Qi, H. Zhang, H. Xu, Application of Unscented Kalman Filter in GPS /INS, 2012, Symposium on Photonics and Optoelectronics, 2012, Shanghai, China, pp.1-3.
9. F. Sun, L.J. Tang, INS/GPS integrated navigation filter algorithm based on cubature Kalman filter, 2012, Control and Decision, vol. 27, no. 7, pp.1032-1036.

10. F. Sun, L.J. Tang, Improved particle filter algorithm for INS/GPS integrated navigation system, 2011, International Conference on Mechatronics & Automation, Beijing, China, pp.2392-2396.
11. S. Bhaumik, Swati, Cubature quadrature kalman filter, 2015, International Journal of Control, Automation and systems, vol. 7, no.5, pp.533-541.
12. M. Kiani, S.H. Pourtakdoust, Adaptive square-root cubature-quadrature Kalman particle filter via KLD-sampling for orbit determination, 2015, Aerospace Science & Technology, no. 46, pp.159-167.
13. Y.C. Hou, W.C. Penf, Distance between uncertain random variables, 2014, Mathematical Modelling of Engineering Problems, vol. 1, no. 1, pp.15-20.
14. W. Wei, Y.Y. Qin, X.D. Zhang, Y.C. Zhang, Comparative Analysis of H-infinity Filtering in INS/GPS Integrated Navigation Application, 2012, Journal of Xian Technological University, vol. 32, no. 11, pp.874-855.
15. H.K. Sahoo, P.K. Dash, Robust estimation of power quality disturbances using unscented H-∞ filter, 2015, Electrical Power and Energy Systems, no. 73, pp.438-447.
16. Y.R. Chen, J.P. Yuan, An Improved Robust H-∞ Multiple Fading Fault tolerant Filtering Algorithm for INS/ GPS Integrated Navigation, 2009, Journal of Astronautics, vol. 30, no. 3, pp.930-936.